

THE DISTRIBUTION OF NEARBY STARS IN PHASE SPACE MAPPED BY HIPPARCOS:
THE POTENTIAL WELL AND LOCAL DYNAMICAL MASS

M. Crézé^{1,2}, E. Chereul¹, O. Bienaymé¹, C. Pichon³

¹Observatoire de Strasbourg, CNRS URA1280, 11, rue de l'Université, F-67000 Strasbourg, France

²IUP de Vannes, 8,rue Montaigne, BP 561, 56017 Vannes Cedex, France

³Astronomisches Institut Univ. Basel, Venusstrasse 7, CH-4102 Binningen, Switzerland

ABSTRACT

Hipparcos data provide the first, volume limited and absolute magnitude limited homogeneous tracer of stellar density and velocity distributions in the solar neighbourhood. The density of A-type stars more luminous than $M_v = 2.5$ can be accurately mapped within a sphere of 125 pc radius, while proper motions in galactic latitude provide the vertical velocity distribution near the galactic plane. The potential well across the galactic plane is traced practically hypothesis-free and model-free. The local dynamical density comes out as $\rho_0 = 0.076 \pm 0.015 M_\odot \text{ pc}^{-3}$ a value well below all previous determinations leaving no room for any disk shaped component of dark matter.

Key words: Galaxy: kinematics and dynamics, disc density.

1. INTRODUCTION

The paramount contribution of Hipparcos to astrophysics is to provide direct geometric distances to stars. That is to tie firmly astrophysics to laboratory physics. Not only does it bring some individuals, some stars of such or such kind, but it also brings a full probe of them within a well defined volume, at their due positions and with their due motion. All stars more luminous than a certain limit are measured within a certain limiting distance. This is in a sense a 'Galaxy sample return'.

The starting idea of this investigation was simply this: for the first time we get a sample probe of this strange collisionless gaz which molecules are stars. We get an instant view of the density-velocity equilibrium of well defined tracers in the galaxy potential: a snapshot of the phase space. Let us try and look at it with fresh minds.

There were and there are still mysteries in the behaviour of this gas. It is collisionless yet the stellar velocity dispersion grows with age. It has extremely short typical mixing time, yet there are suggestions

of old velocity groups. In a poster of this volume: Chereul et al. 1997, we give preliminary results of this fresh look based on wavelett analysis.

The first step in this analysis Crézé et al. 1997 of the kinetic equilibrium of the stellar fluid refers to a good old question: the determination of the local volume density. This problem is well known in galactic dynamics; it is usually referred to as 'the K_z problem', where K_z means the force law perpendicular to the galactic plane. The K_z determination and subsequent derivation of the local mass density ρ_0 has a long history, nearly comprehensive reviews can be found in Kerr & Lynden-Bell 1986 covering the subject before 1984 and in Kuijken 1995 since 1984. Early ideas were given by Kapteyn (1922), while Oort (1932) produced the first tentative determination.

The essence of this determination is quite simple: the kinetic energy of stellar motions in the z direction when stars cross the plane fixes their capability to escape away from the potential well. Given a stellar population at equilibrium in this well, its density law $\nu(z)$ and velocity distribution at plane crossing $f(w_0)$ are tied to each other via the K_z or the potential $\phi(z)$. Under quite general conditions the relation that connects both distributions is strictly expressed by Equation 1:

$$\nu(\phi) = 2 \int_{\sqrt{2\phi}}^{\infty} \frac{f(|w_0|) w_0 dw_0}{\sqrt{w_0^2 - 2\phi}} \quad (1)$$

Given $\nu(z)$ and $f(w_0)$, $\phi(z)$ can be derived. Then according to Poisson equation, the local dynamical density comes out as:

$$\rho_0 = \frac{1}{4\pi G} (d^2\phi/dz^2) \quad (2)$$

2. THE LOCAL MISSING MASS ISSUE

Early determinations of ρ_0 (Oort 1960) were as high as $0.18 M_\odot \text{ pc}^{-3}$ while the total mass density of stars and interstellar matter would not exceed $0.08 M_\odot \text{ pc}^{-3}$. The discrepancy between these two

figures latter re-emphasised by J. Bahcall and collaborators (1984ab, 1992), came into the picture of the dark matter controversy to make it even darker. While the local density of standard ‘dark halos’ required to maintain flat rotation curves of galaxies away from their center would hardly exceed 0.01, such ten times larger densities could only be accounted for in rather flat components which composition and origin could not be the same. Following Bahcall’s claim, several attempts were made to reduce the intrinsic inaccuracy of the dynamical mass determinations in particular Bienaymé et al. 1987, used a complete modelisation of the galaxy evolution to tie the K_z determination to star counts, Kuijken & Gilmore 1989 used distant tracers of K type stars to determine not the local volume density but the integrated surface density below 1 kpc, Flynn & Fuchs 1994 pointed at difficulties in relation with the underlying dynamical approach. Most concluded that there was no conclusive evidence for a high dynamical density if all causes of errors were taken into account.

The local mass density of observable components (the observed mass) can hardly exceed $0.08 M_{\odot} \text{pc}^{-3}$ out of which a half stands for stars which local luminosity function is reasonably well known. The mass density of interstellar gas and dust is not so easily accessed since the bulk of it, molecular hydrogen, can only be traced via CO and the ratio CO/H₂ is not so well established. Also interstellar components are basically clumpy and distances poorly known: it is not so easy to define a proper volume within which a density makes sense. A conservative range for the observed mass density should be [0.06, 0.10] including 0.04 for stars.

Nevertheless, so far the discrepancy used to be charged to the dynamical density since the determination of this quantity involved many difficulties, most poorly controlled:

- tracer homogeneity: first of all, the determination require that a suitable tracer can be duly identified. A criterion independent of velocity and distance should allow to detect and select all stars matching the tracer definition. This was hardly achieved by spectral surveys which completeness and selectivity degrade as magnitude grows;
- stationarity: in order for the tracer to make dynamical sense, it should be in equilibrium in the potential. Youngest stars which velocities reflect the kinematics of the gas at their birth time do not fulfill this requirement;
- undersampling: one searches for the bending of density laws caused by gravitation along the z direction. This imposes not only that tracer densities can be determined, but also that they can be determined at scales well below the typical length of the bending. This means that the tracer should be dense enough in the region studied. Most determinations so far rely upon sample surveys in the galactic polar caps, resulting in ‘pencil beam’ samples quite inappropriate to trace the density near the plane (Crézé et al. 1989). When the bending is traced at large distances from the plane as in Kuijken & Gilmore

1989, one gets information on the surface density below a certain height. A comparison of this surface density with the local volume density involves modeling hypotheses. Another associated effect can be generated by a clumpy distribution of the tracer even stationary if the tracer includes clusters or clumps the statistics of densities and velocities may be locally biased. Other problems arise from the velocity distribution sampling;

- systematic errors: out of necessity before Hipparcos, all previous studies used photometric distances. Uncertainties in the calibration of absolute magnitudes resulted in systematic errors in density determinations. This is particularly true for red giants which are not at all a physically homogeneous family and show all but normal absolute magnitude distributions: it is striking that calibrations based on different samples provide discrepant calibrations outside the range permitted by formal errors. This produced both biased density distributions and uncontrolled effects in selecting volume limited samples;
- random errors: distances and velocities were also affected by random measurement errors. Even perfectly calibrated, standard errors of photometric distances based on intermediate band photometry would hardly get below 20 per cent.

Hipparcos data solve nearly all the problems quoted above: instead of ‘pencil beam’ tracers at high galactic latitudes which distribution is only indirectly related to the local K_z , what we get here is a dense probe inside the potential well.

The samples were preselected within magnitude limits inside the completeness limit of the Hipparcos survey program (Turon & Crifo 1986). It includes all stars brighter than $m_v = 8.0$ (7.9 at low latitudes) with spectral types earlier than G0, stars with no or poorly defined spectral types were included provisionally.

Within this coarse preselection, sample stars were eventually selected on the basis of their Hipparcos derived distance, magnitude and colour. So the only physical criterion is absolute magnitude while the sample is distance limited on the basis of individual parallaxes. Within 125 parsecs, Hipparcos parallaxes provide individual distances with accuracies better than 10 percent for over ninety percent of the sample. Distances are individual and free from calibration errors. Samples are dense, typical inter-star distances are less than 10 pc. This is suitable to trace density variations which typical scales are of the order of hundred parsecs. Thanks to this high tracer density, difficulties related to clumpiness can be monitored through appropriate analysis of local density residuals. Stationarity considerations can also be monitored since W velocities are available for stars everywhere in the volume studied.

Three samples have been extracted from the above mentioned pre-selection of A-F-type stars, h125 limited to stars more luminous than $V = 2.5$ (complete to 125 pc), H100 limited to stars more luminous than $V = 3$ (complete to 100 pc) and H80 ($V = 3.5$, 80 pc).

3. MAPPING THE POTENTIAL WELL

Whatever the velocity distribution, once a homogeneous tracer has been defined, i.e. once a selection criterion has been defined uncensored with respect to velocities and positions, Equation 1 expresses the correspondence between the tracer density law and the potential as a plain change of variables. If there is a potential well present in the data, it must appear as a density peak. If we can map the density trend model free, we will get a picture of the potential well.

The tracer should be dense enough for the typical distances between tracer stars to be small with respect to the typical scale of density variations. Under this assumption, at a place where the tracer density is ν , the observed number of stars in any probe volume V is a Poisson variate with expectation $V \cdot \nu$. Defining v as the single star volume around one specific star (that is the sphere extending to the nearest neighbour), and introducing the quantity $x = v \cdot \nu$ we get a new variate whose expectation is 1 and whose probability distribution is exponential (Equation 3). It is the probability distribution of the distance between two events in a Poisson process under unit density:

$$dP(x) = \exp(-x) dx \quad (3)$$

and the probability distribution of the single star volume v is:

$$dP(v) = \nu \cdot \exp(-\nu \cdot v) dv \quad (4)$$

so the expectation of the single star volume is $1/\nu$, which makes it a suitable local statistics for the density. It is not a novel approach to use statistics based on nearest-neighbour distances to investigate densities, but it is appropriate here since it turns out to provide a parameter-free ML estimator for the density by plain moving average of single star volumes.

Single star volumes which are unbiased local estimates of the inverse tracer density have been computed for all the tracer samples described above. Defining x, y, z as a set of cartesian coordinates centered at the sun position, with z positive pointing towards $b = +90^\circ$, x positive towards the galactic center ($l = 0^\circ$) and y towards $l = 90^\circ$, each series of values was sorted along x , y and z successively and each resulting set smoothed by moving average along the sort parameter. Single star volumes are averaged over 101 neighbouring stars, producing parameter free maximum likelihood inverse density profiles. Figures 1 show the resulting profiles along x , y and z for our most accurate and extended sample (namely samples h125).

At first glance only do the h125 profile along the z axis show significant bending. This is a direct mapping of the potential well. Edge effects potentially related to completeness and/or to distance errors can be easily controlled: would they be responsible for the main part of the observed bending they would appear as well on the x and y plots. There is no such thing visible even at marginal level. In addition, any significant incompleteness at the edges would result in a density decrease driving the single star volume statistics up at the edges. As a result, the dynamical density derived below, once corrected for this effect, would be even smaller.

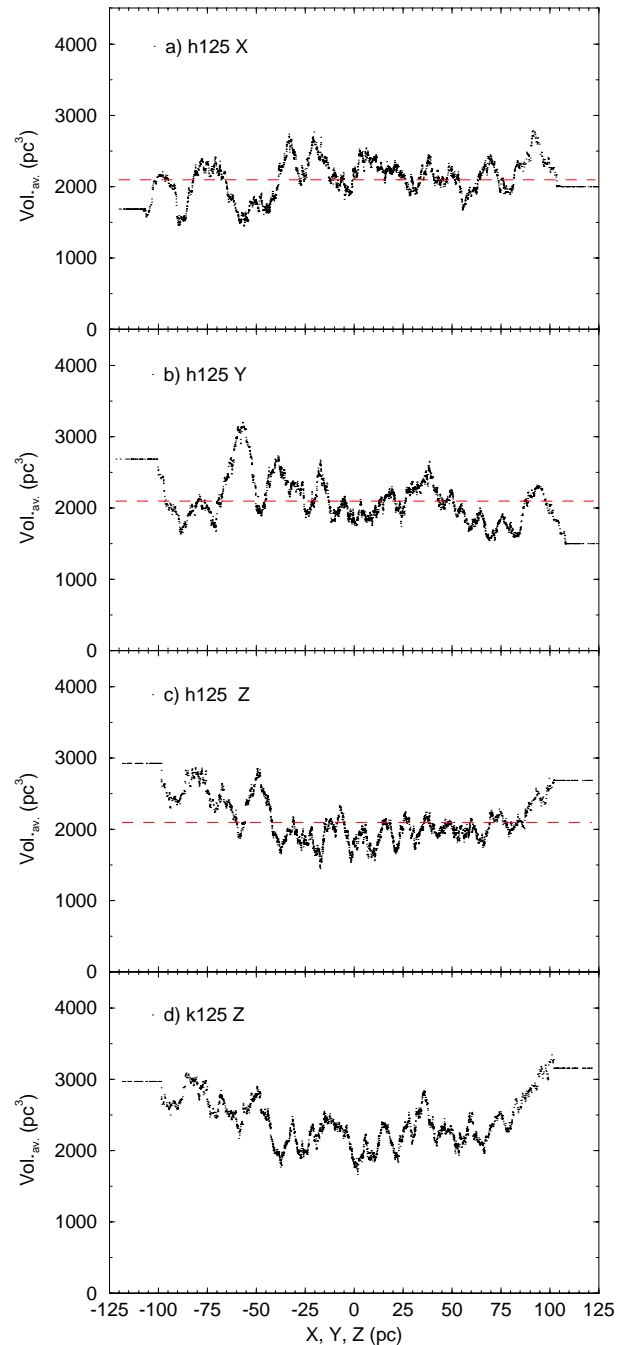


Figure 1. Single star volumes for A stars with $M_v \leq 2.5$ within 125 pc (sample h125) volumes in cubic parsecs are moving averaged along (a) the x ($l = 0$, $b = 0$); (b) y ($l = 90$, $b = 0$); and (c) z ($b = 90$) directions. Moving averages are performed over 101 stars, so that random fluctuations are roughly one order of magnitude below that of raw data. (d) shows in comparison the same kind of plot for sample k125 axis z , where cluster stars have been removed from sample h125. The bending due to the potential well in the galactic plane is clearly visible on plots c and d.

Table 1. Maximum likelihood solutions for the local dynamical density from the three Hipparcos samples.

Sample	N	z_0 pc	β	σ_{w1} km s ⁻¹	σ_{w2} km s ⁻¹	$1/\nu_0$ (\star/pc^3) ⁻¹	ρ_0 M_\odot/pc^3	Likelihood
h125	2977	12.0 (6.0)	0.50	10.67 (0.31)	6.08 (0.27)	1887.67 (35.63)	0.075 (0.009)	-25666.64
H100	2677	4.0 (9.0)	0.50	12.49 (0.46)	6.39 (0.63)	1061.13 (20.65)	0.089 (0.017)	-21511.41
H80	2336	13.0	0.50	14.46 (0.63)	6.60 (0.68)	631.57 (13.20)	0.076 (0.028)	-17485.54

4. ESTIMATING ρ_0

Solving Eqs. (1) and (2) for $\phi(z)$ can follow two different ways: a parametric approach and a non-parametric one. Either were used on the above defined samples producing quite similar results:

- in the parametric approach, realistic mathematical forms are adopted for both $\phi(z)$ and $f(w_0)$. Free parameters for $f(w_0)$ can be determined by fitting the observed vertical velocity distribution then adopting $f(w_0)$ free parameters for the potential, $\phi(z)$ can be derived from the observed density. The advantage of this approach is simplicity in so far as manageable formulae can be found to represent $f(w_0)$. The cost is that results may be biased by the choice of the model. An advantage may be that systematic effects can be traced and individual residuals can be computed at the position and velocity of each star. Table 1 summarizes the the results of maximum like lihood solutions obtained from the three samples described above following this approach. The velocity distributions were approximated by fitting a double gaussian model;
- at the other end one can try to produce a purely numerical fit. Since this kind of fit is unstable to noise in the data, some regularization should be applied. This non-parametric approach has been also used.

The results of Maximum Likelihood solutions obtained in the parametric approach on the basis of a double gaussian model for the W velocity distributions are summarized in Table 1. The accuracy of determinations based on eldest samples with highest velocity dispersions, presumably well mixed suffers from the small z range spanned. Nevertheless all solutions point towards very low values of the local density ρ_0 . This result is fully conforted by non-parametric determinations showing that it does not depend on the adopted mathematical form for the velocity distribution.

The consequence of these estimations is to fix the total mass density in the galactic disc in the neighbourhood of the Sun in the range 0.065–0.10 $M_\odot \text{pc}^{-3}$ with a most probable value by 0.076 $M_\odot \text{pc}^{-3}$. In conclusion we review below the consequences of this very low value in terms of local dynamical mass versus observed density, in terms of global galaxy modelling and in terms of dark matter distribution. Under the resulting potential the theoretical density

trend of each sample accross the galactic plane can be derived from the corresponding velocity distribution. This is shown on Figure 2 overlotted on corresponding observed density profiles. Models with substantially higher densities are obviously rejected.

5. DYNAMICAL MASS VERSUS KNOWN MATTER

Previous dynamical determinations of the local mass density used to be based on star counts a few hundred parsecs away from the galactic plane providing constraints for the local column density integrated over a substantial layer. Comparisons were tentatively made with the observed density of known galactic components, namely visible stellar populations, stellar remnants, ISM. So, on either side of the comparison there were assumptions on the vertical distribution of matter involved.

For the first time, the present determination is based on strictly local data inside a sphere of more than 100 parsecs radius and gives access directly to the total mass density around the Sun in the galactic plane.

On the side of the known matter, 0.085 $M_\odot \text{pc}^{-3}$ is probably an acceptable figure. But the uncertainty is larger than 0.02. It does not make sense to overcomment about the observed mass density being larger than the dynamical estimate: for one thing the discrepancy is far below the error bars, for the other thing there has been little effort dedicated so far to estimate properly the smallest density compatible with observations, the attention being always focused on upper bounds. For the moment the only conclusion is that the density of known matter has a lower limit of say 0.065 $M_\odot \text{pc}^{-3}$. In term of mass discrepancy controversy, the main uncertainty is now on the observation side.

Trying to build a dynamical model of the galactic disc compatible with these values, we get some clarification of the dark halo controversy.

A good convergence is now obtained on the main parameters of the disc populations although there is no agreement as to the exact decomposition in populations (see for example, Reid & Gilmore 1983, Robin et al 1986ab-1996, Haywood 1997ab, Gould et al. 1996, etc.). The tentative structural parameters of our model are close to Gould's (see also Sackett 1997): stellar disc scale length 2.5 kpc, scale height 323 pc; thick disc scale length 3.5 kpc, scale

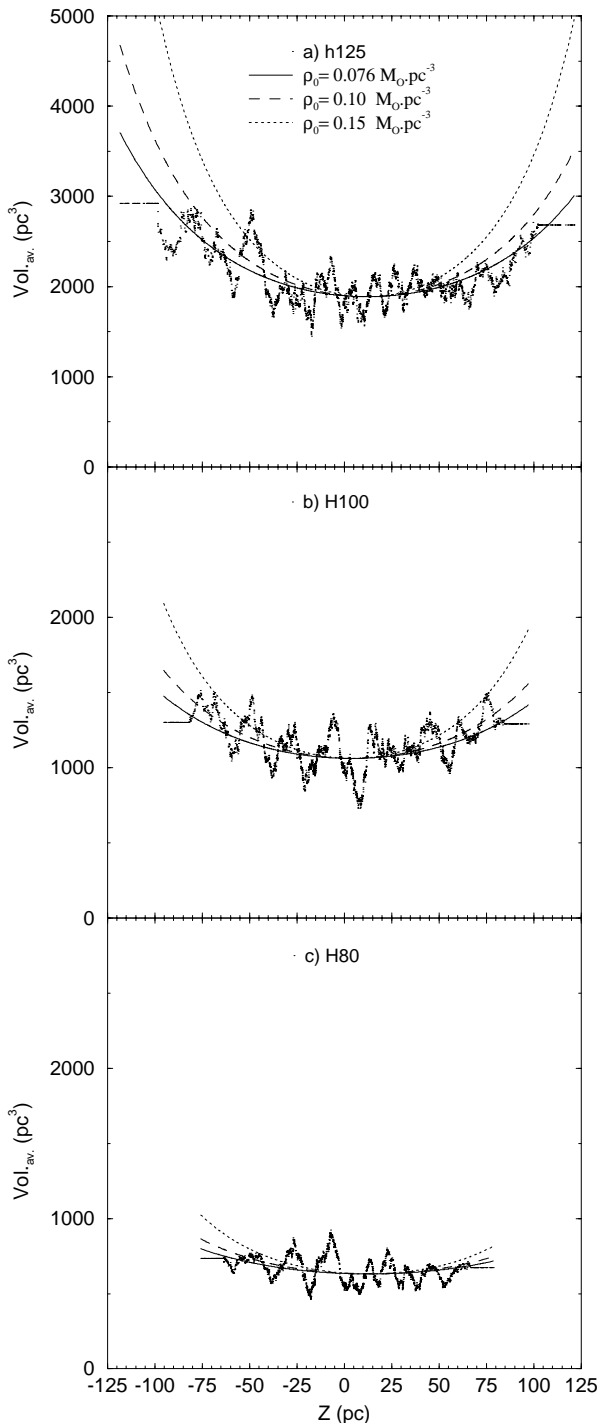


Figure 2. Calculated inverse density profiles under three different assumed values of the local mass density $0.076 M_{\odot} \text{pc}^{-3}$ (best estimate), $0.10 M_{\odot} \text{pc}^{-3}$ and $0.15 M_{\odot} \text{pc}^{-3}$ (from bottom to top on each plot). Based on the velocity distributions of sample h125 (a), H100 (b) and H80 (c).

height (exponential) 656 pc. 20 per cent of the local stellar density is in the thick disc. The error on the scale length has little effect on the disc mass M_d : $M_d(2.5 \text{ kpc})/M_d(3.5 \text{ kpc}) = 1.34$ (assuming $R_0 = 8.5 \text{ kpc}$) and a factor 1.26 on the amplitude of the corresponding velocity curves.

Adopting a total stellar mass density $\rho_* = 0.043 M_{\odot} \text{pc}^{-3}$, the surface density at R_0 is then $\Sigma_0 = 33.4 M_{\odot} \text{pc}^{-2}$.

The contributions of the bulge and stellar halo are small beyond 3 kpc of the galactic center. They are neglected in this discussion.

The interstellar matter is accounted for by a double exponential disc 2500/80 pc its local density is set to $0.04 M_{\odot} \text{pc}^{-3}$.

The total column density due to gas and stellar component is $\Sigma_0 = 40 M_{\odot} \text{pc}^{-2}$.

A dark halo is necessary to maintain a flat rotation curve beyond the solar galactic radius. It is modeled with a Miyamoto spheroid that allows flattening.

This mass model is fitted to the rotation curve setting the solar galactic radius to $R_0=8.5 \text{ kpc}$ and the velocity curve at R_0 to 220 km s^{-1} . The velocity curve is assumed flat beyond 5 kpc of the center to 20 kpc.

The first consequence is that the stellar disc (stars+remnants+gas) does not contribute for more than half the mass implied by the rotation curve at $R_0=8.5 \text{ kpc}$: the galactic disc is far from maximal. Even with $R_0=7.5 \text{ kpc}$, a maximal disc would mean a rotation curve plateau as low as 164 km s^{-1} . This is excluded by inner HI and CO rotation curves.

Filling the galactic mass distribution with a strictly spherical dark matter halo required by the rotation curve, the dark matter local density comes out as $\rho_{\text{dark halo}}(R_0, z=0) = 0.007 M_{\odot} \text{pc}^{-3}$. Such a local density of dark matter is well compatible with the above quoted uncertainties of the dynamical and known mass. However, any attempt to flatten the mass distribution of the dark component result in an increase of the local halo density. Under the most extreme hypotheses, that is considering the interstellar matter contribution negligible and giving the stellar component a total density $0.043 M_{\odot} \text{pc}^{-3}$ with the same scale length and adopting our best dynamical estimate at its face value (0.076) the acceptable halo scale height cannot go below 2150 pc.

So, there is just room for a spherical halo (local density: $0.008 M_{\odot} \text{pc}^{-3}$). Extreme changes of the parameters are needed to permit a significantly flatter dynamical halo. There is no room for an important amount of dark matter in the disc. Dark matter models assuming that the dark matter is in form of a flat component related to a flat fractal ISM should be modified to equivalent models where dark matter is in form of fractal structures distributed in the halo (Pfenniger et al 1994ab, Gerhard & Silk 1996).

6. CONCLUSIONS

We presently conclude:

1. the potential well across the galactic plane has been traced practically hypothesis-free and model-free, it turns out to be shallower than expected;
2. the local dynamical volume density comes out as $0.076 \pm 0.015 M_{\odot} \text{ pc}^{-3}$ a value well compatible with all existing observations of the known matter;
3. building a disc-thick disc mass model compatible with this constraint as well as previous determinations of the local surface density, it is shown that such a disc cannot be maximal, a massive halo of dark matter is required;
4. the dark halo should be spherical or nearly spherical in order for its local density to remain within the range permitted between the known matter density and the current determination of the dynamical density;
5. there is no room left for any disk shaped component of dark matter.

REFERENCES

- Arenou, F., Lindegren, L., Froeschle, F., Gomez, A.E., Turon, C., Perryman, M.A.C, Wielen, R., 1995, *A&A*, 304, 52.
- Bahcall, J.N., 1984a, *ApJ*, 276, 169
- Bahcall, J.N., 1984b, *ApJ*, 287, 926
- Bahcall, J.N., Flynn, C., Gould, A., 1992, *ApJ*, 389, 234
- Bienaymé, O., Robin, A.C., Crézé, M., 1987, *A&A*, 180, 94
- Chereul, E., Crézé, M., Bienaymé, O., 1997, *ESA SP-402*, this volume
- Combes, F., 1991, *ARAA*, 29, 195
- Crézé, M., Robin, A.C., Bienaymé, O., 1989, *A&A*, 211, 1
- Crézé, M., Chereul, E., Bienaymé, O., Pichon, C. 1997, *A&A*, submitted
- ESA, 1992, *The Hipparcos Input Catalogue*, *ESA SP-1136*
- ESA, 1997, *The Hipparcos and Tycho Catalogues*, *ESA SP-1200*
- Flynn C., Fuchs B., 1994, *MNRAS*, 270, 471
- Fuchs B., Wielen R., 1993, *Back to the Galaxy*, eds Holt & Verter, 580
- Gerhard O., Silk J., 1996, *ApJ*, 472, 34
- Gould A., Bahcall J.N., Flynn C., 1996, *ApJ*, 465, 759
- Haywood, M., Robin, A.C, Crézé, M., 1997a, *A&A*, 320, 428
- Haywood, M., Robin, A.C, Crézé, M., 1997b, *A&A*, 320, 440
- Ishida, K., Mikami, T., Nogushi, T., Maehara, H., 1982, *PASJ*, 34, 381
- Kapteyn, J.C., 1922, *ApJ*, 55, 302
- Kerr, F.J., Lynden-Bell, D., 1986, *MNRAS*, 221, 1023
- Kuijken K., Gilmore, G., 1989, *MNRAS*, 239, 650
- Kuijken, K., 1995, *Stellar populations*, *IAU Symp.* 164, 195
- Oort, J.H., 1932, *BAN*, 6, 249
- Oort, J.H., 1960, *BAN*, 15, 45
- Pichon, C., Thiébaud, E., 1997, *MNRAS*, submitted
- Pfenniger, D., Combes, F., Martinet, L., 1994a, *A&A*, 285, 79
- Pfenniger, D., Combes, F., 1994b, *A&A*, 285, 94
- Ratnatunga, K.U., Casertano, S., 1991, *AJ*, 101, 1075
- Reid, N., Gilmore, G., 1983, *MNRAS*, 202, 1025
- Reid, N., Hawley, S. L., Gizis, J.E., 1995, *AJ*, 110(4), 1838
- Robin, A.C., Crézé, M., 1986a, *A&A*, 157, 71
- Robin, A.C., Crézé, M., 1986b, *A&AS*, 64, 53
- Robin, A.C., Haywood, M., Crézé, M., Ojha, D.K., Bienaymé, O., 1996, *A&A*, 305, 125
- Turon, C., Crifo, F., 1986, in: 'IAU Highlights of Astronomy', Vol. 7, Swings J.P. (ed.), 683
- Sackett, P.D., 1997, *ApJ*, in press
- Sion, E.M., Liebert, J.W., 1977, *ApJ*, 213, 468
- Wahba, G., Wendelberger, J., 1979, *Monthly Weather Review*, 108, 1122
- Wielen, R., Jahreiss, H., Kruger, R., 1983, *The nearby stars and the stellar luminosity function*, *IAU Coll.* 76, 163